

4.7.2 Influence of surface roughness on shear strength

Shear tests carried out on **smooth, clean discontinuity** surfaces at constant normal stress generally give shear stress-shear displacement curves of the type shown in Figure 4.35.

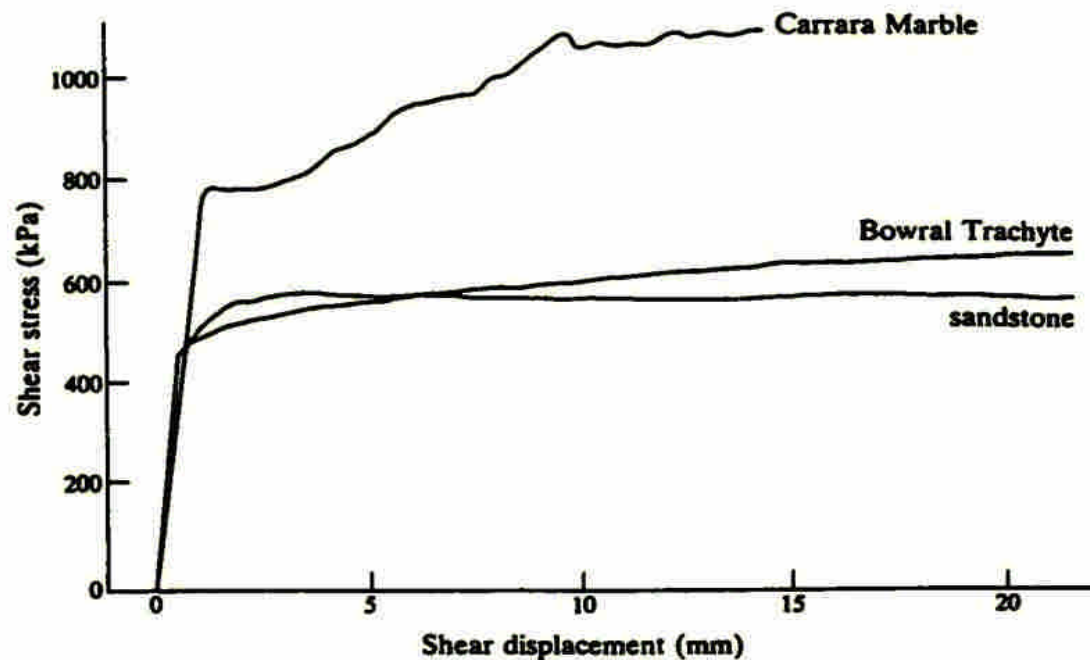


Figure 4.35 Shear stress-shear displacement curves for ground surfaces tested with a constant normal stress of 1.0 MPa (after Jaeger, 1971).

4.7.2 Influence of surface roughness on shear strength

When a number of such tests are carried out at a range of effective normal stresses, a **linear shear strength envelope** is obtained.

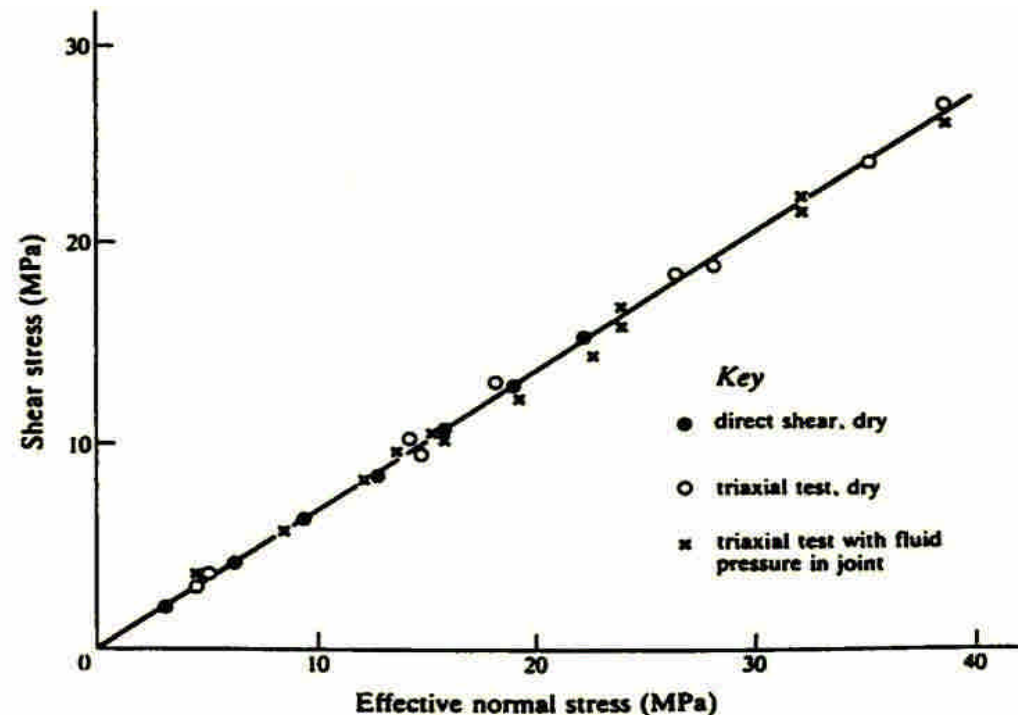
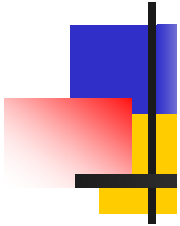


Figure 4.36 Sliding of smooth quartzite surfaces under various conditions (after Jaeger and Rosen-gren, 1969).

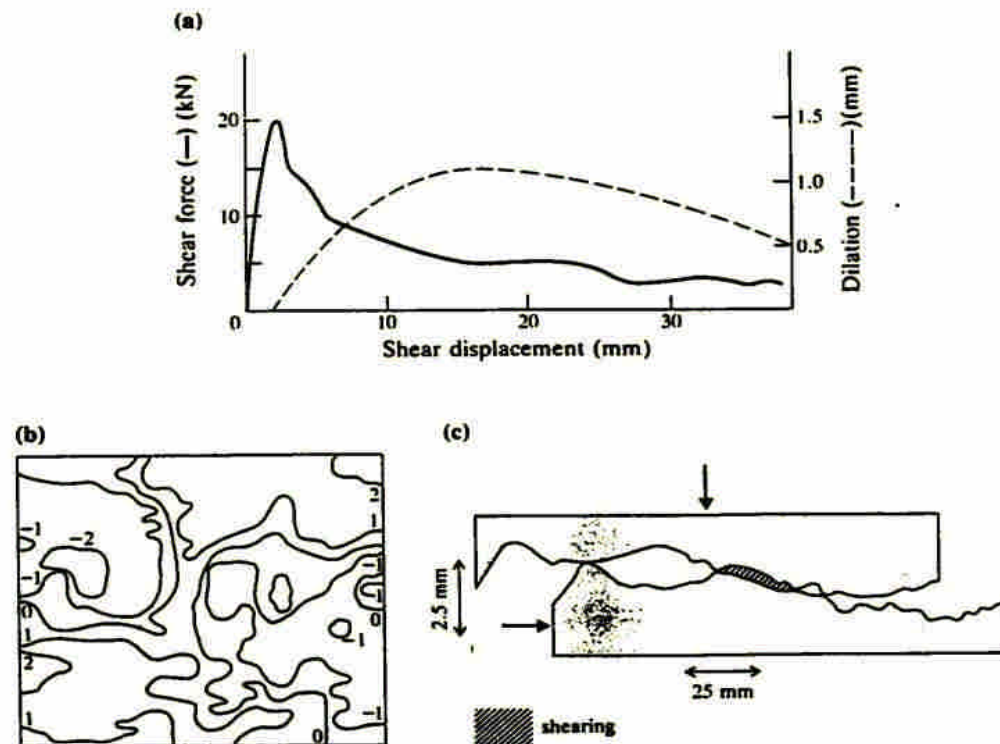
4.7.2 Influence of surface roughness on shear strength

The shear strength of **smooth, clean discontinuities** can be described by the **simple Coulomb law** where ϕ is the effective angle of friction of the discontinuity surfaces.

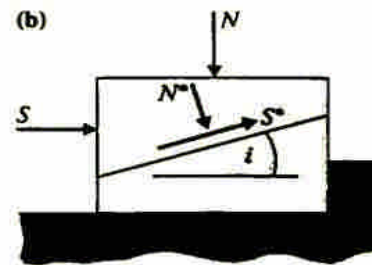
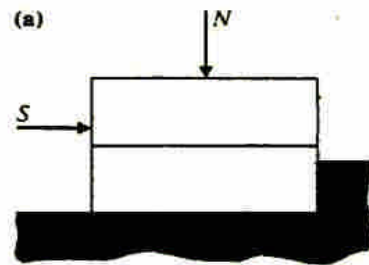


The **shear force- shear displacement** curve shown in Figure 4.37a is typical of the results obtained for clean, **rough** discontinuities. The peak strength at constant normal stress is reached after a small shear displacement. With further displacement, the shear resistance falls until the residual strength is eventually reached.

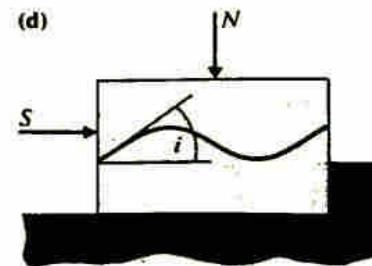
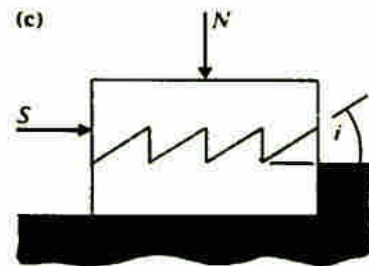
Figure 4.37 Results of a direct shear test on a 127 mm × 152 mm graphite-coated joint, carried out at a constant normal force of 28.9 kN. (a) Shear force-shear displacement curves; (b) surface profile contours before testing (mm); (c) relative positions on a particular cross section after 25 mm of sliding (after Jaeger, 1971).



4.7.2 Influence of surface roughness on shear strength



$$\frac{S}{N} = \tan \phi_{\text{effective}}$$



$$\frac{S^*}{N^*} = \tan \phi \quad (4.32)$$

Figure 4.39 Idealised surface roughness models illustrating the roughness angle, i .

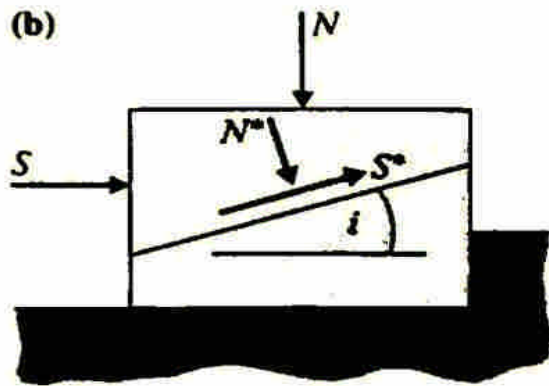
and

$$S^* = S \cos i - N \sin i$$

$$N^* = N \cos i + S \sin i$$

$$\frac{S}{N} = \tan(\phi + i) \quad (4.33)$$

Derive Eq. 4.33



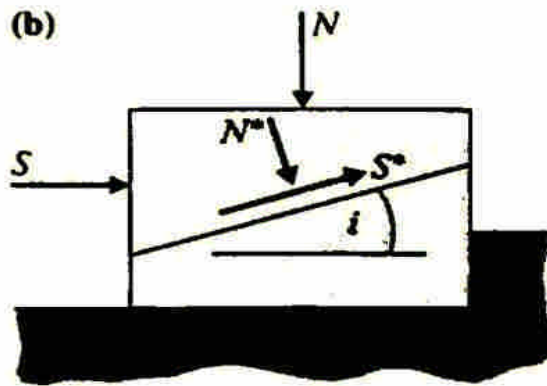
$$S^* = S \cos i - N \sin i$$

$$N^* = N \cos i + S \sin i$$

$$\frac{S^*}{N^*} = \tan \phi = \frac{S \cos i - N \sin i}{N \cos i + S \sin i}$$

$$S(\cos i - \sin i \tan \phi) = N(\cos i \tan \phi + \sin i)$$

Influence of surface roughness on shear strength



$$\frac{S}{N} = \frac{\cos i \tan \phi + \sin i}{\cos i - \sin i \tan \phi}$$

Dividing the numerator and denominator by $\cos i$, gives

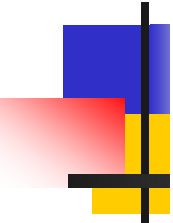
$$\frac{S}{N} = \frac{\tan \phi + \tan i}{1 - \tan i \tan \phi}$$

$$\tan(\alpha + \beta) = \frac{\tan \alpha + \tan \beta}{1 - \tan \alpha \tan \beta}$$

$$= \tan(\phi + i)$$

4.7.2 Influence of surface roughness on shear strength

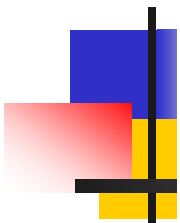
Thus the inclined discontinuity surface has an **apparent friction angle** of $(\phi + i)$.



Patton extended this model to include the case in which the discontinuity surface contains a number of

'teeth' (Figure 4.39c and d). In a series of model experiments with a variety of surface profiles, he found that, at **low values of N** , sliding on the inclined surfaces occurred **according to equation 4.33**.

4.7.2 Influence of surface roughness on shear strength



Dilation of the specimens necessarily accompanied this mechanism. As the value of **N was increased** above some critical value, sliding on the inclined **asperity surfaces** was inhibited, and a value of **S** was eventually reached at which **shear failure** through the **asperities** occurred

4.7.2 Influence of surface roughness on shear strength

The corresponding values of S and N gave the upper portion of the **bilinear shear strength envelope** shown in Figure 4.40.

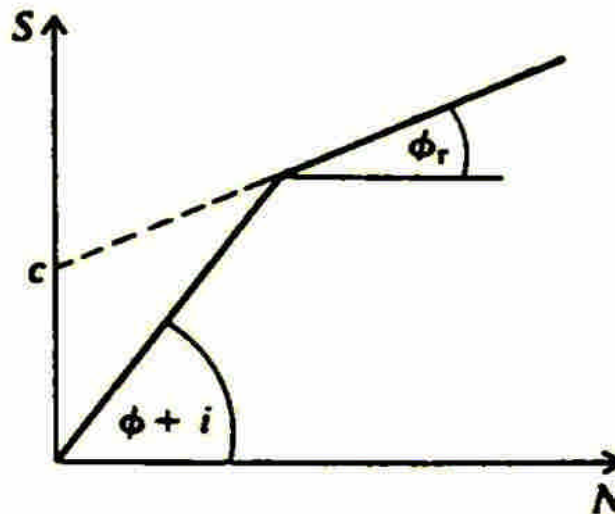
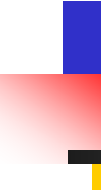


Figure 4.40 Bilinear peak strength envelope obtained in direct shear tests on the models shown in Figure 4.39.

4.7.2 Influence of surface roughness on shear strength

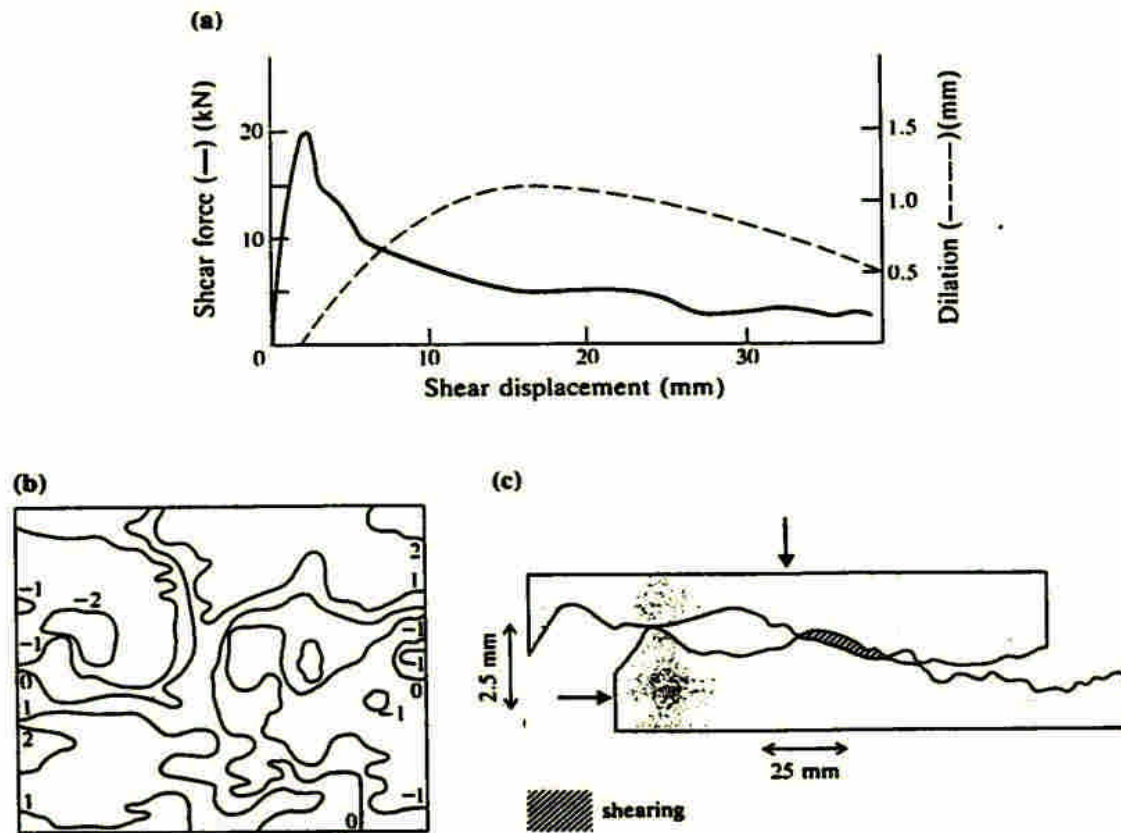


Natural discontinuities rarely behave in the same way as these idealised models. However, the same two mechanisms - sliding on inclined surfaces at low normal loads and the suppression of dilation and shearing through asperities at higher normal loads - are found to dominate natural discontinuity behaviour.

Generally, the two mechanisms are combined in varying proportions with the result that peak shear strength envelopes do not take the idealised bilinear form of Figure 4.40 but are curved.

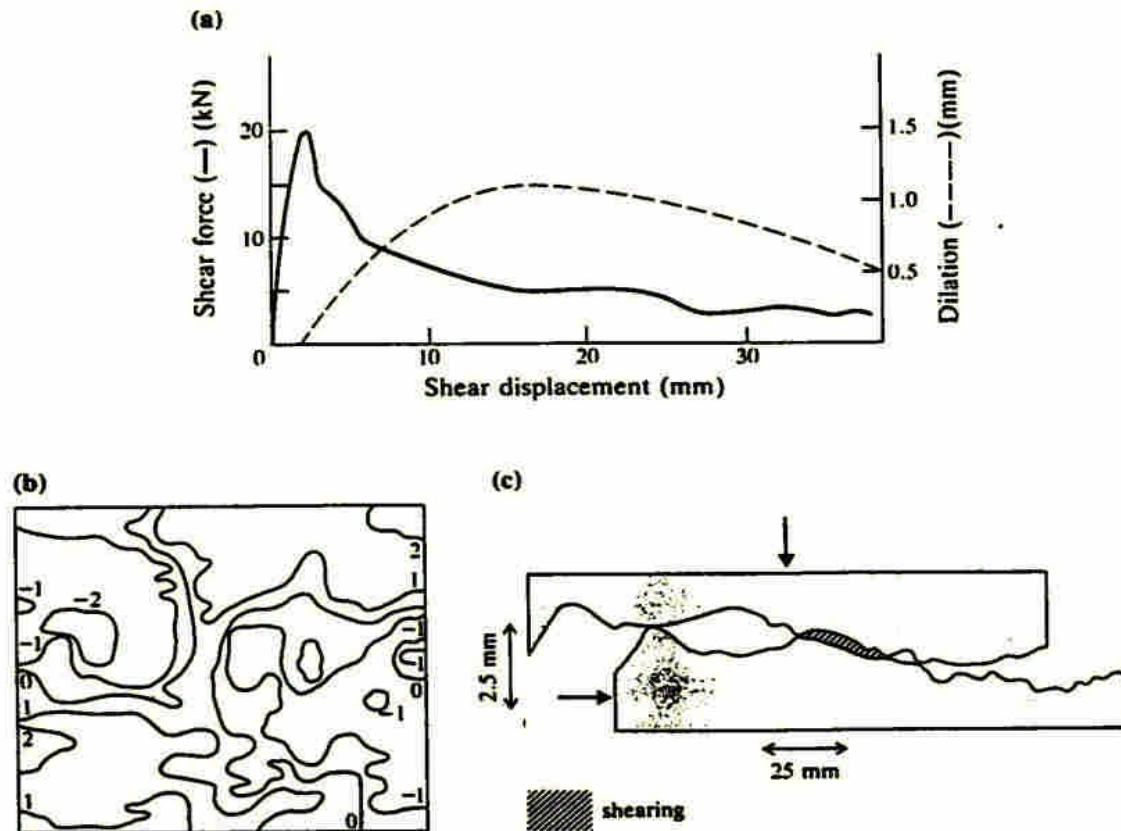
These combined effects are well illustrated by the direct shear test on a **graphite-coated joint** which gave the results shown in Figure 4.37a. The roughness profile of the initially mating surfaces is shown in Fig 4.37b.

Figure 4.37 Results of a direct shear test on a 127 mm × 152 mm graphite-coated joint, carried out at a constant normal force of 28.9 kN. (a) Shear force–shear displacement curves; (b) surface profile contours before testing (mm); (c) relative positions on a particular cross section after 25 mm of sliding (after Jaeger, 1971).



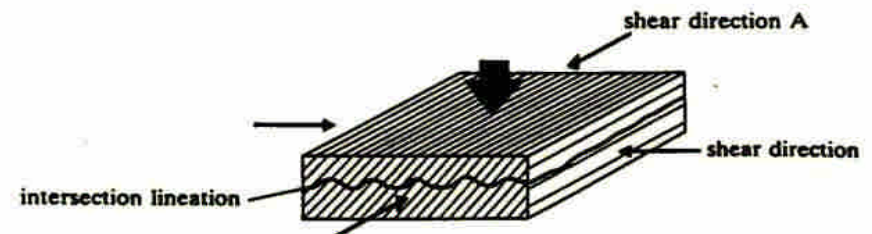
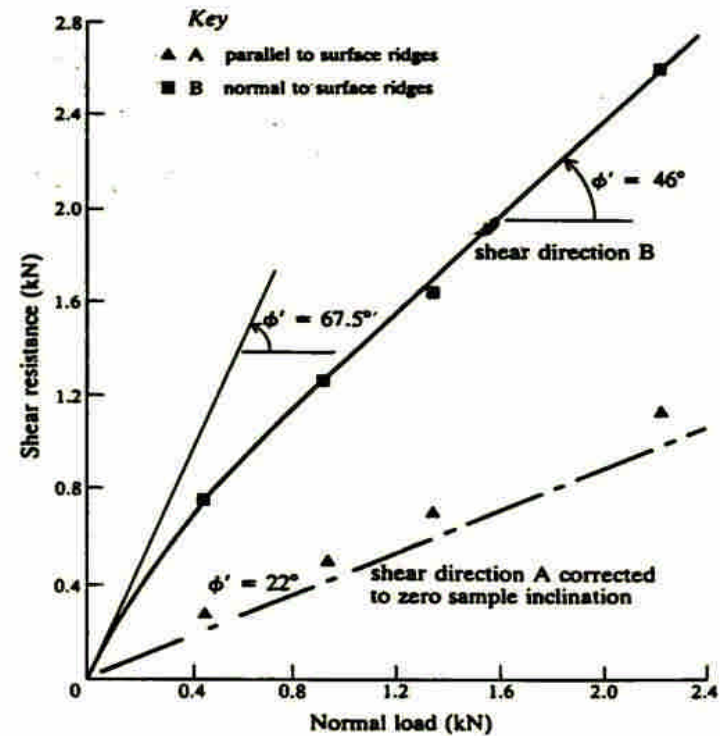
The maximum departure from the mean plane over the 127 mm x 152 mm surface area was in the order of ± 2.0 mm. After 25 mm of shear displacement at a constant normal force of 28.9 kN, the relative positions of the two parts of the specimen were as shown in Figure 4.37c.

Figure 4.37 Results of a direct shear test on a 127 mm x 152 mm graphite-coated joint, carried out at a constant normal force of 28.9 kN. (a) Shear force–shear displacement curves; (b) surface profile contours before testing (mm); (c) relative positions on a particular cross section after 25 mm of sliding (after Jaeger, 1971).



Roughness effects can cause shear strength to be a directional property. Figure 4.41 illustrates a case in which **rough discontinuity surfaces** were prepared in slate specimens by fracturing them at a constant angle to the cleavage.

Figure 4.41 Effect of shearing direction on the shear strength of a wet discontinuity in a slate (after Brown *et al.*, 1977).

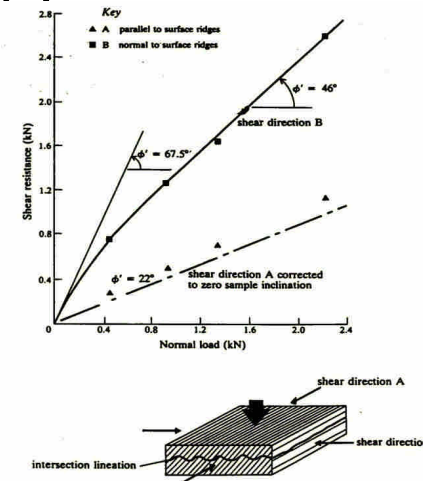


4.7.2 Influence of surface roughness on shear strength

When the specimens were tested in direct shear with the directions of the ridges on the surfaces parallel to the direction of sliding (test A), the resulting shear strength

envelope gave an effective friction angle of 22° which compares with a value of 19.5° obtained for clean, polished surfaces. normal stress.

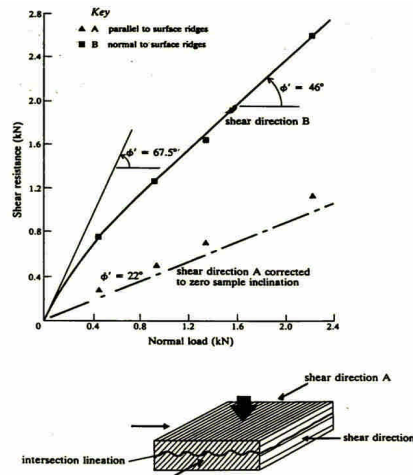
Figure 4.41 Effect of shearing direction on the shear strength of a wet discontinuity in a slate (after Brown *et al.*, 1977).



4.7.2 Influence of surface roughness on shear strength

However, when the shearing direction was normal to the ridges (**test B**), sliding up the ridges occurred with attendant dilation. A curved shear strength envelope was obtained with a **roughness angle** of 45.5° at near zero effective normal stress and a roughness angle of 24° at **higher values** of effective normal stress.

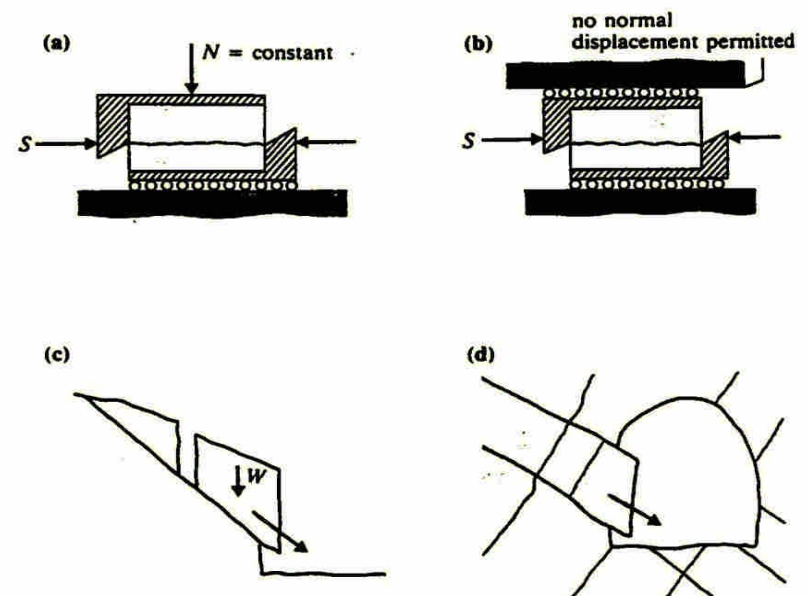
Figure 4.41 Effect of shearing direction on the shear strength of a wet discontinuity in a slate (after Brown *et al.*, 1977).



4.7.3 Interrelation between dilatancy and shear strength

- Goodman (1976) pointed out that **controlled normal force shear test** although test may reproduce discontinuity behaviour adequately in the case of sliding of an unconstrained block of rock from a slope (Figure 4.42c).

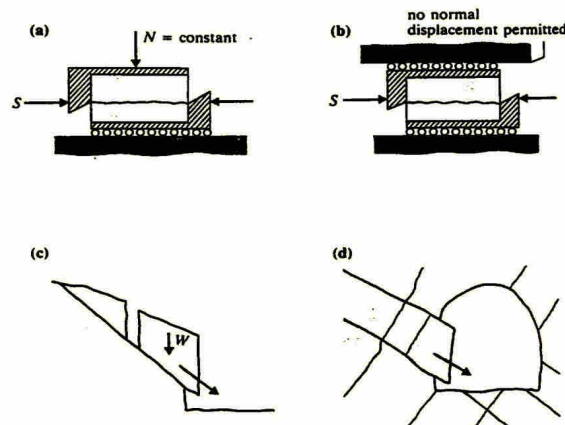
Figure 4.42 Controlled normal force (a, c) and controlled normal displacement (b, d) shearing modes.



4.7.3 Interrelation between dilatancy and shear strength

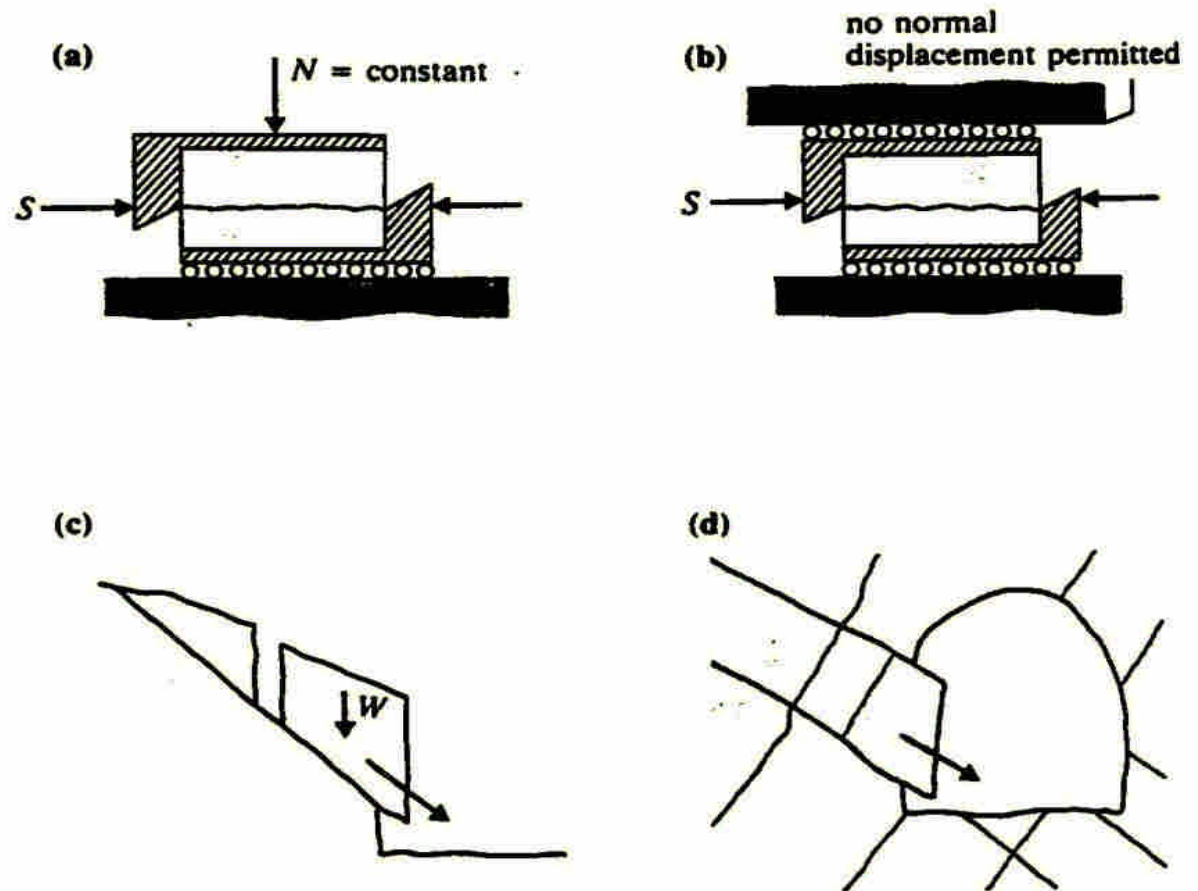
- The **controlled normal force shear test** may not be suited to the determination of the stress-displacement behaviour of discontinuities isolating a block that may potentially slide or fall from the periphery of an underground excavation (Figure 4.42d).

Figure 4.42 Controlled normal force (a, c) and controlled normal displacement (b, d) shearing modes.



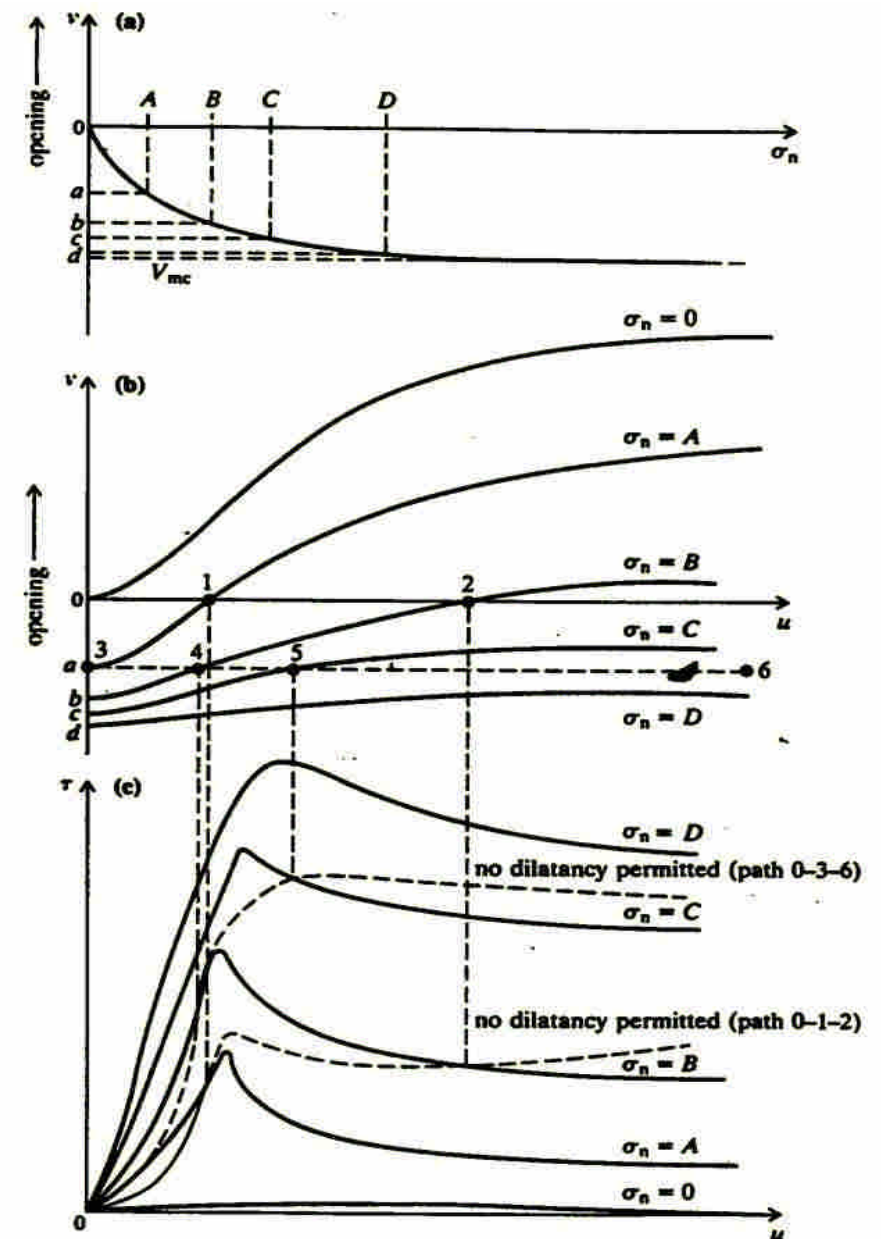
4.7.3 Interrelation between dilatancy and shear strength

Figure 4.42 Controlled normal force (a, c) and controlled normal displacement (b, d) shearing modes.



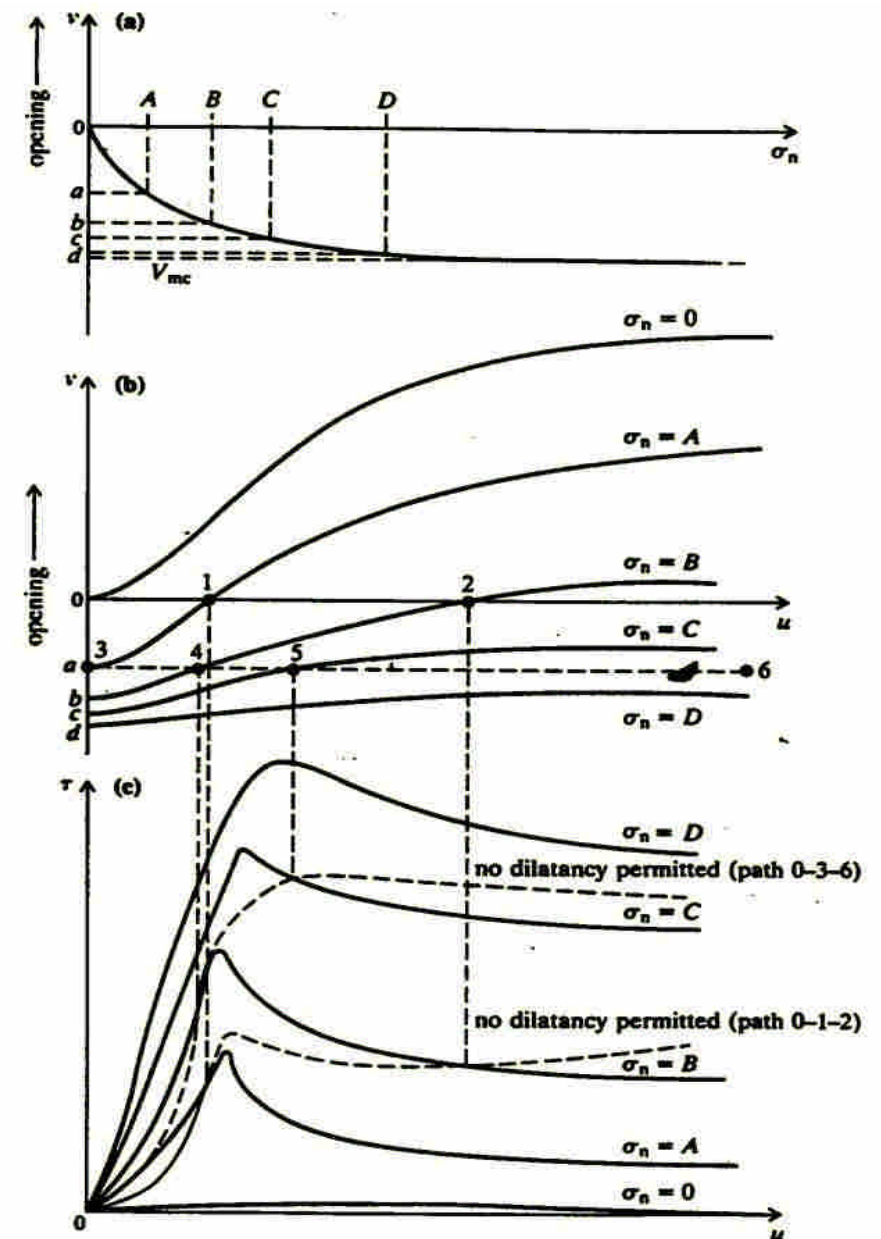
When a normal compressive stress, σ_n , is applied, the discontinuity will compress. This compressive stress-displacement behaviour is highly non-linear (Figure 4.43a) and at high values of σ_n , becomes asymptotic to a maximum closure. V_{mc} , related to the initial thickness or aperture of the discontinuity.

Figure 4.43 Relations between normal stress (σ_n), shear stress (τ), normal displacement (v), and shear displacement (u) in constant displacement shear tests on rough discontinuities (after Goodman, 1980).



Suppose that a clean, rough discontinuity is sheared with no normal stress applied. Dilatancy will occur as shown in the upper curve of Figure 4.43b. If the shear resistance is assumed to be solely frictional, the shear stress will be zero throughout.

Figure 4.43 Relations between normal stress (σ_n), shear stress (τ), normal displacement (v), and shear displacement (u) in constant displacement shear tests on rough discontinuities (after Goodman, 1980).



For successively higher values of constant normal stress, A, B, C and D, the initial normal displacement will be a, b, c and d as shown in Figure 4.43a,

and the dilatancy-shear displacement and shear stress-shear displacement curves

obtained during shearing will be as shown in Figures 4.43b and c.

normal stress (σ_n), shear stress (τ), normal displacement (v), and shear displacement (u) in constant displacement shear tests on rough discontinuities (after Goodman, 1980).

